Measurement of Differential Branching Fractions of Inclusive $B \to X_u \ell^+ \nu_\ell$ Decays

L. Cao,[1,8,*] W. Sutcliffe,[1] R. Van Tonder,[1] F. U. Bernlochner,[1,†] I. Adachi,[18,14] H. Aihara,[83] D. M. Asner,[3] T. Aushev,[20] R. Ayad,[91] V. Babu,[8] S. Bahinipati,[24] P. Behera,[26] K. Belous,[30] J. Bennett,[54] M. Bessner,[17] T. Bilka,[5] J. Biswal,[35] A. Bobrov,[4,63] M. Bračko,[51,35] P. Branchini,[32] T. E. Browder,[17] A. Budano,[32] M. Campajola,[31,56] D. Červenkov,[5] M.-C. Chang,[10] P. Chang,[59] B. G. Cheon,[16] K. Chilikin,[45] H. E. Cho,[16] K. Cho,[40] S.-J. Cho,[90] Y. Choi,[76] S. Choudhury,[25] D. Cinabro,[88] S. Cunliffe,[8] T. Czank,[37] N. Dash,[26] G. De Pietro,[32] R. Dhamija,[25] F. Di Capua,[31,56] J. Dingfelder,[1] Z. Doležal,[5] T. V. Dong,[11] S. Dubey,[17] D. Epifanov,[4,63] T. Ferber,[8] D. Ferlewicz,[53] A. Frey,[13] B. G. Fulsom,[65] R. Garg,[66] V. Gaur,[87] N. Gabyshev,[4,63] A. Garmash,[4,63] A. Giri,[25] P. Goldenzweig,[36] T. Gu,[68] K. Gudkova,[4,63] S. Halder,[78] T. Hara,[18,14] O. Hartbrich,[17] K. Hayasaka,[62] M. Hernandez Villanueva,[8] W.-S. Hou,[59] C.-L. Hsu,[77] K. Inami,[55] A. Ishikawa,[18,14] R. Itoh,[18,14] M. Iwasaki,[64] W. W. Jacobs,[27] E.-J. Jang,[15] S. Jia,[11] Y. Jin,[83] K. K. Joo,[6] J. Kahn,[36] K. H. Kang,[43] H. Kichimi,[18] C. Kiesling,[52] C. H. Kim,[16] D. Y. Kim,[75] S. H. Kim,[73] Y.-K. Kim,[90] T. D. Kimmel,[87] K. Kinoshita,[7] P. Kodyš,[5] T. Konno,[39] A. Korobov,[4,63] S. Korpar,[51,35] E. Kovalenko,[4,63] P. Križan,[47,35] R. Kroeger,[54] P. Krokovny,[4,63] T. Kuhr,[48] R. Kulasiri,[38] M. Kumar,[50] R. Kumar,[69] K. Kumara,[88] A. Kuzmin,[4,63] Y.-J. Kwon,[90] S. C. Lee,[43] C. H. Li,[46] J. Li,[43] L. K. Li,[7] Y. B. Li,[67] L. Li Gioi,[52] J. Libby,[26] K. Lieret,[48] D. Liventsev,[88,18] C. MacQueen,[53] M. Masuda,[82,70] M. Merola,[31,56] F. Metzner,[36] K. Miyabayashi,[57] R. Mizuk,[45,20] G. B. Mohanty,[78] S. Mohanty,[78,86] M. Mrvar,[29] M. Nakao,[18,14] A. Natochii,[17] L. Nayak,[25] M. Niiyama,[42] N. K. Nisar,[3] S. Nishida,[18,14] K. Nishimura,[17] S. Ogawa,[80] H. Ono,[61,62] Y. Onuki,[83] P. Oskin,[45] G. Pakhlova,[20,45] S. Pardi,[31] H. Park,[43] S.-H. Park,[18] A. Passeri,[32] S. Patra,[23] S. Paul,[79,52] T. K. Pedlar,[49] L. E. Piilonen,[87] T. Podobnik,[47,35] V. Popov,[20] E. Prencipe,[21] M. T. Prim,[1] M. Röhrken,[8] A. Rostomyan,[8] N. Rout,[26] M. Rozanska,[60] G. Russo,[56] D. Sahoo,[78] S. Sandilya,[25] A. Sangal,[7] L. Santelj,[47,35] T. Sanuki,[81] V. Savinov,[68] G. Schnell,[2,22] J. Schueler,[17] C. Schwanda,[29] A. J. Schwartz,[7] Y. Seino,[62] K. Senyo,[89] M. E. Sevior,[53] M. Shapkin,[30] C. Sharma,[50] C. P. Shen,[11] J.-G. Shiu,[59] B. Shwartz,[4,63] F. Simon,[52] A. Sokolov,[30] E. Solovieva,[45] M. Starič,[35] J. F. Strube,[65] M. Sumihama,[12] T. Sumiyoshi,[85] M. Takizawa,[74,19,71] U. Tamponi,[33] K. Tanida,[34] Y. Tao,[9] F. Tenchini,[8] K. Trabelsi,[44] M. Uchida,[84] T. Uglov,[45,20] S. Uno,[18,14] P. Urquijo,[53] S. E. Vahsen,[17] G. Varner,[17] K. E. Varvell,[77] E. Waheed,[18] C. H. Wang,[58] E. Wang,[68] M.-Z. Wang,[59] P. Wang,[28] X. L. Wang,[11] M. Watanabe,[62] S. Watanuki,[44] O. Werbycka,[60] E. Won,[41] B. D. Yabsley,[77] W. Yan,[72] S. B. Yang,[41] H. Ye,[8] J. H. Yin,[41] Z. P. Zhang,[72] V. Zhilich,[4,63] and V. Zhukova[45]

(Belle Collaboration)

[1]*University of Bonn, 53115 Bonn*
[2]*Department of Physics, University of the Basque Country UPV/EHU, 48080 Bilbao*
[3]*Brookhaven National Laboratory, Upton, New York 11973*
[4]*Budker Institute of Nuclear Physics SB RAS, Novosibirsk 630090*
[5]*Faculty of Mathematics and Physics, Charles University, 121 16 Prague*
[6]*Chonnam National University, Gwangju 61186*
[7]*University of Cincinnati, Cincinnati, Ohio 45221*
[8]*Deutsches Elektronen–Synchrotron, 22607 Hamburg*
[9]*University of Florida, Gainesville, Florida 32611*
[10]*Department of Physics, Fu Jen Catholic University, Taipei 24205*
[11]*Key Laboratory of Nuclear Physics and Ion-beam Application (MOE) and Institute of Modern Physics, Fudan University, Shanghai 200443*
[12]*Gifu University, Gifu 501-1193*
[13]*II. Physikalisches Institut, Georg-August-Universität Göttingen, 37073 Göttingen*
[14]*SOKENDAI (The Graduate University for Advanced Studies), Hayama 240-0193*
[15]*Gyeongsang National University, Jinju 52828*
[16]*Department of Physics and Institute of Natural Sciences, Hanyang University, Seoul 04763*
[17]*University of Hawaii, Honolulu, Hawaii 96822*
[18]*High Energy Accelerator Research Organization (KEK), Tsukuba 305-0801*
[19]*J-PARC Branch, KEK Theory Center, High Energy Accelerator Research Organization (KEK), Tsukuba 305-0801*
[20]*National Research University Higher School of Economics, Moscow 101000*
[21]*Forschungszentrum Jülich, 52425 Jülich*
[22]*IKERBASQUE, Basque Foundation for Science, 48013 Bilbao*
[23]*Indian Institute of Science Education and Research Mohali, SAS Nagar, 140306*

[24]Indian Institute of Technology Bhubaneswar, Satya Nagar 751007
[25]Indian Institute of Technology Hyderabad, Telangana 502285
[26]Indian Institute of Technology Madras, Chennai 600036
[27]Indiana University, Bloomington, Indiana 47408
[28]Institute of High Energy Physics, Chinese Academy of Sciences, Beijing 100049
[29]Institute of High Energy Physics, Vienna 1050
[30]Institute for High Energy Physics, Protvino 142281
[31]INFN–Sezione di Napoli, I-80126 Napoli
[32]INFN–Sezione di Roma Tre, I-00146 Roma
[33]INFN–Sezione di Torino, I-10125 Torino
[34]Advanced Science Research Center, Japan Atomic Energy Agency, Naka 319-1195
[35]J. Stefan Institute, 1000 Ljubljana
[36]Institut für Experimentelle Teilchenphysik, Karlsruher Institut für Technologie, 76131 Karlsruhe
[37]Kavli Institute for the Physics and Mathematics of the Universe (WPI), University of Tokyo, Kashiwa 277-8583
[38]Kennesaw State University, Kennesaw, Georgia 30144
[39]Kitasato University, Sagamihara 252-0373
[40]Korea Institute of Science and Technology Information, Daejeon 34141
[41]Korea University, Seoul 02841
[42]Kyoto Sangyo University, Kyoto 603-8555
[43]Kyungpook National University, Daegu 41566
[44]Université Paris-Saclay, CNRS/IN2P3, IJCLab, 91405 Orsay
[45]P.N. Lebedev Physical Institute of the Russian Academy of Sciences, Moscow 119991
[46]Liaoning Normal University, Dalian 116029
[47]Faculty of Mathematics and Physics, University of Ljubljana, 1000 Ljubljana
[48]Ludwig Maximilians University, 80539 Munich
[49]Luther College, Decorah, Iowa 52101
[50]Malaviya National Institute of Technology Jaipur, Jaipur 302017
[51]Faculty of Chemistry and Chemical Engineering, University of Maribor, 2000 Maribor
[52]Max-Planck-Institut für Physik, 80805 München
[53]School of Physics, University of Melbourne, Victoria 3010
[54]University of Mississippi, University, Mississippi 38677
[55]Graduate School of Science, Nagoya University, Nagoya 464-8602
[56]Università di Napoli Federico II, I-80126 Napoli
[57]Nara Women's University, Nara 630-8506
[58]National United University, Miao Li 36003
[59]Department of Physics, National Taiwan University, Taipei 10617
[60]H. Niewodniczanski Institute of Nuclear Physics, Krakow 31-342
[61]Nippon Dental University, Niigata 951-8580
[62]Niigata University, Niigata 950-2181
[63]Novosibirsk State University, Novosibirsk 630090
[64]Osaka City University, Osaka 558-8585
[65]Pacific Northwest National Laboratory, Richland, Washington 99352
[66]Panjab University, Chandigarh 160014
[67]Peking University, Beijing 100871
[68]University of Pittsburgh, Pittsburgh, Pennsylvania 15260
[69]Punjab Agricultural University, Ludhiana 141004
[70]Research Center for Nuclear Physics, Osaka University, Osaka 567-0047
[71]Meson Science Laboratory, Cluster for Pioneering Research, RIKEN, Saitama 351-0198
[72]Department of Modern Physics and State Key Laboratory of Particle Detection and Electronics, University of Science and Technology of China, Hefei 230026
[73]Seoul National University, Seoul 08826
[74]Showa Pharmaceutical University, Tokyo 194-8543
[75]Soongsil University, Seoul 06978
[76]Sungkyunkwan University, Suwon 16419
[77]School of Physics, University of Sydney, New South Wales 2006
[78]Tata Institute of Fundamental Research, Mumbai 400005
[79]Department of Physics, Technische Universität München, 85748 Garching
[80]Toho University, Funabashi 274-8510
[81]Department of Physics, Tohoku University, Sendai 980-8578
[82]Earthquake Research Institute, University of Tokyo, Tokyo 113-0032

[83]*Department of Physics, University of Tokyo, Tokyo 113-0033*
[84]*Tokyo Institute of Technology, Tokyo 152-8550*
[85]*Tokyo Metropolitan University, Tokyo 192-0397*
[86]*Utkal University, Bhubaneswar 751004*
[87]*Virginia Polytechnic Institute and State University, Blacksburg, Virginia 24061*
[88]*Wayne State University, Detroit, Michigan 48202*
[89]*Yamagata University, Yamagata 990-8560*
[90]*Yonsei University, Seoul 03722*
[91]*Department of Physics, Faculty of Science, University of Tabuk, Tabuk 71451*

(Received 29 July 2021; accepted 9 November 2021; published 22 December 2021)

The first measurements of differential branching fractions of inclusive semileptonic $B \to X_u \ell^+ \nu_\ell$ decays are performed using the full Belle data set of 711 fb^{-1} of integrated luminosity at the $\Upsilon(4S)$ resonance and for $\ell = e, \mu$. With the availability of these measurements, new avenues for future shape-function model-independent determinations of the Cabibbo-Kobayashi-Maskawa matrix element $|V_{ub}|$ can be pursued to gain new insights in the existing tension with respect to exclusive determinations. The differential branching fractions are reported as a function of the lepton energy, the four-momentum-transfer squared, light-cone momenta, the hadronic mass, and the hadronic mass squared. They are obtained by subtracting the backgrounds from semileptonic $B \to X_c \ell^+ \nu_\ell$ decays and other processes, and corrected for resolution and acceptance effects.

DOI: 10.1103/PhysRevLett.127.261801

In this Letter, we present the first measurements of the differential branching fractions of inclusive semileptonic $B \to X_u \ell^+ \nu_\ell$ decays, obtained from analyzing the full Belle data set of 711 fb^{-1} of integrated luminosity at the $\Upsilon(4S)$ resonance and for $\ell = e, \mu$. The measured distributions can be used for future studies of the nonperturbative decay dynamics of $B \to X_u \ell^+ \nu_\ell$ transitions, and novel determinations of the b-quark mass m_b and of the Cabibbo-Kobayashi-Maskawa (CKM) matrix element $|V_{ub}|$. The presented measurements use the same collision events that were analyzed in Ref. [1]. Therein, partial branching fractions of charmless semileptonic decays were reported using an analysis technique relying on the full reconstruction of the second B meson of the $e^+e^- \to \Upsilon(4S) \to B\bar{B}$ process. This approach allows for the direct reconstruction of the four momentum of the hadronic X system of the $B \to X_u \ell^+ \nu_\ell$ process and other kinematic quantities of interest. The analysis strategy of the presented measurements follows Ref. [1], but more stringent selection criteria are applied to improve the resolution of key variables and further suppress backgrounds from $B \to X_c \ell^+ \nu_\ell$ decays and other processes. Charge conjugation is implied throughout this Letter and $B \to X_u \ell^+ \nu_\ell$ is defined as the average branching fraction of B^+ and B^0 meson decays.

Differential branching fractions are reported as a function of the lepton energy in the signal B rest frame E_ℓ^B, the invariant mass M_X and mass squared M_X^2 of the hadronic X system, the four-momentum-transfer squared $q^2 = (p_B - p_X)^2$ of the B to the lepton and neutrino system, and the two light-cone momenta $P_\pm = (E_X^B \mp |\mathbf{p}_X^B|)$ with E_X^B and $\mathbf{p}_X^B$ in the signal B rest frame. Measurements of these distributions are of great interest as they allow for the study of nonperturbative shape functions [2]. Shape functions describe the Fermi motion of the b quark inside the B meson, and enter in the calculation of the dynamics of $B \to X_u \ell^+ \nu_\ell$ decays. Currently, properties of the leading-order $\Lambda_{\mathrm{QCD}}/m_b$ shape function can only be studied using the photon energy spectrum of $B \to X_s \gamma$ decays and moments of the lepton energy or hadronic invariant mass in charmed semileptonic B decays [3–5]. The modeling of both the leading and subleading shape functions introduce large theory uncertainties on predictions of the $B \to X_u \ell^+ \nu_\ell$ decay rate, and hence on the determination of $|V_{ub}|$. With the presented differential branching fractions, we provide the necessary experimental input for future model-independent approaches, whose aim is to reduce this model dependence by directly measuring the shape function [6,7]. This will lead to more reliable determinations of $|V_{ub}|$ from inclusive processes and give new insights into the persistent tension with the values obtained from exclusive determinations [8] of about 3 standard deviations.

We analyze $(772 \pm 10) \times 10^6$ B meson pairs recorded at the $\Upsilon(4S)$ resonance energy and 79 fb^{-1} of collision events recorded 60 MeV below the $\Upsilon(4S)$ peak, which were both recorded at the KEKB e^+e^- collider [9] by the Belle detector. Belle is a large-solid-angle magnetic spectrometer and a detailed description of its subdetectors and performance can be found in Ref. [10]. Monte Carlo (MC) samples of B meson decays and continuum processes ($e^+e^- \to q\bar{q}$ with $q = u, d, s, c$) are simulated using the `EvtGen` generator [11] and a detailed description of all samples and models is given in Ref. [1]. The simulated samples are used for the background subtraction and to correct for detector resolution, selection, and acceptance effects. The sample sizes used correspond to approximately ten and five times, respectively, the Belle collision data for B meson production and continuum processes. Semileptonic $B \to X_u \ell^+ \nu_\ell$ decays are modeled as a mixture of specific exclusive modes and nonresonant contributions using a so-called "hybrid" approach [12], following closely the implementation of [13,14]. In the hybrid approach, the triple differential rate of the inclusive and combined exclusive predictions are combined such that partial rates of the inclusive prediction are recovered. This is achieved by assigning three dimensional weights to the inclusive contribution as a function of the generator-level q^2, E_ℓ^B, and M_X. For the inclusive contribution, we use two different calculations, i.e. the De Fazio and Neubert (DFN) model [15] and the Bosch-Lange-Neubert-Paz (BLNP) model [16], and treat their difference as a systematic uncertainty. The simulated inclusive $B \to X_u \ell^+ \nu_\ell$ events are hadronized with the JETSET algorithm [17] into final states with two or more mesons. A summary of the used $B \to X_u \ell^+ \nu_\ell$ branching fractions and decay models is given in Table I. Semileptonic $B \to X_c \ell^+ \nu_\ell$ decays are dominated by $B \to D \ell^+ \nu_\ell$ and $B \to D^* \ell^+ \nu_\ell$ decays, which are simulated with form factor parametrizations discussed in Refs. [18–20] and values determined by Refs. [21,22]. The remaining $B \to X_c \ell^+ \nu_\ell$ decays are simulated as a mix of resonant and nonresonant modes, using Ref. [23] for the modeling of $B \to D^{**} \ell^+ \nu_\ell$ form factors. The known difference between inclusive and the sum of measured exclusive $B \to X_c \ell^+ \nu_\ell$ is filled with $B \to D^{(*)} \eta \ell^+ \nu_\ell$ decays.

TABLE I. Semileptonic $B \to X_u \ell^+ \nu_\ell$ decays are modeled as a mixture of specific exclusive modes and nonresonant contributions. The branching fractions are from the world averages from Ref. [24] and the models and form factors (FFs) used are listed. We use natural units ($\hbar = c = 1$).

$\mathcal{B}$	Value B^+	Value B^0
$B \to \pi \ell^+ \nu_\ell$ [a,e]	$(7.8 \pm 0.3) \times 10^{-5}$	$(1.5 \pm 0.06) \times 10^{-4}$
$B \to \eta \ell^+ \nu_\ell$ [b,e]	$(3.9 \pm 0.5) \times 10^{-5}$	$\cdots$
$B \to \eta' \ell^+ \nu_\ell$ [b,e]	$(2.3 \pm 0.8) \times 10^{-5}$	$\cdots$
$B \to \omega \ell^+ \nu_\ell$ [c,e]	$(1.2 \pm 0.1) \times 10^{-4}$	$\cdots$
$B \to \rho \ell^+ \nu_\ell$ [c,e]	$(1.6 \pm 0.1) \times 10^{-4}$	$(2.9 \pm 0.2) \times 10^{-4}$
$B \to X_u \ell^+ \nu_\ell$ [d,e]	$(2.2 \pm 0.3) \times 10^{-3}$	$(2.0 \pm 0.3) \times 10^{-3}$

[a]BCL FFs [25] from fit to LQCD [26] and Ref. [27].
[b]Pole FFs from LCSR [28].
[c]BSZ FFs fit [29] to LCSR [30] and Refs. [31–33].
[d]DFN [15] ($m_b^{\mathrm{KN}} = (4.66 \pm 0.04)$ GeV, $a^{\mathrm{KN}} = 1.3 \pm 0.5$) or BLNP model [16] ($m_b^{\mathrm{SF}} = 4.61$ GeV, $\mu_\pi^{2\,\mathrm{SF}} = 0.20$ GeV^2).
[e]Inclusive and exclusive decays are mixed using hybrid approach [12].

Collision events are reconstructed using the multivariate algorithm of Ref. [34], in which one of the two B mesons is fully reconstructed in hadronic final states (labeled as B_{tag}). Signal candidates are reconstructed by identifying an electron or muon candidate with $E_\ell^B = |\mathbf{p}_\ell^B| > 1$ GeV in the signal B rest frame, and by reconstructing the hadronic X system of the $B \to X_u \ell^+ \nu_\ell$ semileptonic process using charged particles and neutral energy depositions of the collision event not used in the reconstruction of the B_{tag} candidate. The largest background after the reconstruction is from the CKM-favored $B \to X_c \ell^+ \nu_\ell$ process, which possesses a very similar decay signature, completely dominating the selected candidate events. To identify $B \to X_u \ell^+ \nu_\ell$ candidates, eleven distinguishing features are combined into a single discriminant using a multivariate classifier in the form of boosted decision trees (BDTs) using the implementation of Ref. [35]. The most discriminating variables are the reconstructed neutrino mass M_{miss}^2, the vertex fit probability of the $X\ell$ decay vertex, and the number of identified $K^\pm$ and K_S^0 in the X system. To improve the resolution on the reconstructed variables or the signal to background ratio, additional selections are applied. For the measurements involving the hadronic X system (M_X, M_X^2, q^2, $P_\pm$), we demand the missing energy E_{miss} and the magnitude of the missing momentum $|\mathbf{p}_{\mathrm{miss}}|$ of the collision to be consistent with each other by requiring $|E_{\mathrm{miss}} - |\mathbf{p}_{\mathrm{miss}}|| < 0.1$ GeV. This improves the resolution by 21%–37%, depending on the observable, and removes poorly reconstructed events. The signal efficiency after the BDT selection and this additional requirement is 8% while rejecting 99.5% of all $B \to X_c \ell^+ \nu_\ell$ background events, as defined with respect to all selected signal or $B \to X_c \ell^+ \nu_\ell$ events after successfully identifying a suitable B_{tag} candidate. To reduce the contamination of $B \to X_c \ell^+ \nu_\ell$ and other backgrounds, for the measurements of q^2 and the light-cone momenta $P_\pm$, an additional requirement of $M_X < 2.4$ GeV is imposed: this selection, mostly targeting poorly understood high-mass X_c states, removes in addition background from secondary leptons and reduces the $B \to X_c \ell^+ \nu_\ell$ contamination by an additional 20%. The reconstruction resolution of the lepton energy is excellent, thus no requirement on the missing energy and the magnitude of the missing momentum of the event is imposed, but to reduce background contributions we also require $M_X < 2.4$ GeV. This results in a signal efficiency of 17% and 99% of $B \to X_c \ell^+ \nu_\ell$ background events are rejected as defined with respect to all events after the B_{tag} selection.

The differential branching fractions are extracted by subtracting the remaining background contributions from $B \to X_c \ell^+ \nu_\ell$ and other sources in the measured distributions. This is implemented in a four-step procedure: first a binned likelihood fit to the M_X distribution is carried out to estimate the number of background events. The M_X fit takes the shape of signal and background from MC simulations and includes as nuisance parameters systematic effects that can impact the template shapes. To reduce the dependence on the precise modeling of the $B \to X_u \ell^+ \nu_\ell$ process, a coarse binning is used. In particular, the resonance region ($M_X \in [0, 1.5]$ GeV) is described by a single bin. The analyzed hadronic invariant mass spectra with and without the selection on $|E_{\mathrm{miss}} - |\mathbf{p}_{\mathrm{miss}}|| < 0.1$ GeV and the used binning for the different fits are shown in Fig. 1.

In the second step, the background is subtracted using the estimated normalization from the corresponding M_X fit in the kinematic variable under study. The background shape is taken from MC simulation. The statistical uncertainty on the background-subtracted yields are determined using a bootstrapping procedure [36,37] to properly incorporate the correlation from the M_X fit as the same data events are analyzed. The same method is used to determine the statistical correlations between all bins of all measured distributions. The systematic uncertainties associated with modeling the background shape and normalization are also propagated into the uncertainties of the estimated signal yields. In the third step, the signal yields are unfolded using the singular value decomposition (SVD) algorithm from Ref. [38] with the implementation of Ref. [39]. The regularization parameter of the unfolding method was carefully tuned with simulated samples to minimize the dependence on m_b, the shape function modeling, and the composition of the $B \to X_u \ell^+ \nu_\ell$ signal. In the final step the unfolded yields are corrected for efficiency and acceptance effects to the partial phase space defined by $E_\ell^B > 1$ GeV, also correcting for QED final-state radiation. The full analysis procedure was validated with independent MC samples and ensembles of pseudoexperiments and no biases of central values or uncertainties were observed.

Systematic uncertainties from the background subtraction, the modeling of the detector response for $B \to X_u \ell^+ \nu_\ell$, and uncertainties entering the total normalization are consistently propagated through the background subtraction, unfolding, and efficiency correction procedure. For the background subtraction we evaluate $B \to X_u \ell^+ \nu_\ell$ and $B \to X_c \ell^+ \nu_\ell$ modeling (FFs, nonperturbative parameters and composition) and detector related systematic uncertainties. The largest systematic uncertainties are typically from the assumptions entering the modeling of the $B \to X_u \ell^+ \nu_\ell$ signal composition, but depending on

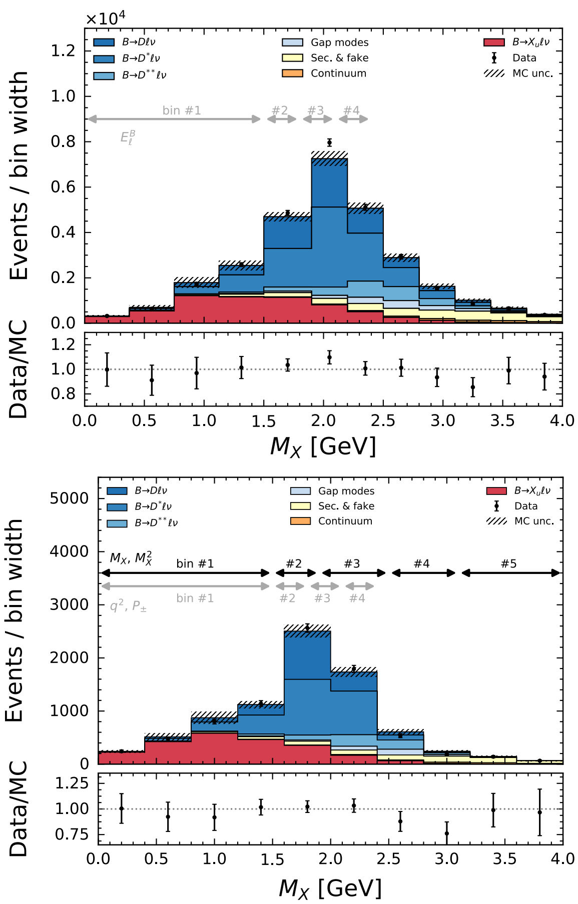

FIG. 1. The reconstructed M_X distributions after the BDT selection without (top) and with (bottom) the requirement of $|E_{\mathrm{miss}} - |\mathbf{p}_{\mathrm{miss}}|| < 0.1$ GeV are shown. The arrows indicate the coarse binning used in the background subtraction fit for the different variables. Removing the $M_X > 2.4$ GeV events improves the signal to background ratio for E_ℓ^B, q^2, and $P_\pm$, but is not necessary for measurements of M_X and M_X^2.

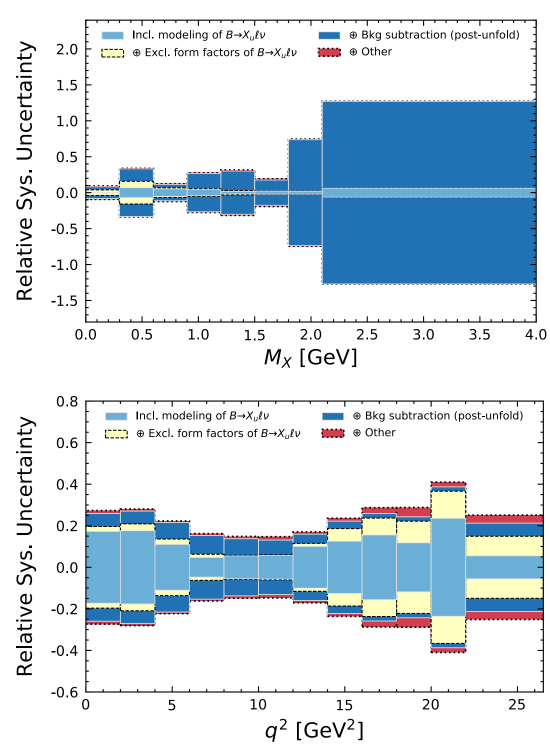

FIG. 2. The relative systematic uncertainties on the unfolded differential branching fraction as a function of M_X and q^2 are shown. The different uncertainty sources are color coded.

the region of phase space also the background subtraction uncertainty can be a dominant source of uncertainty. Figure 2 shows the relative uncertainties on the unfolded differential branching fractions as a function of M_X and q^2. The total systematic uncertainties range from 9% to 130% in relative error, and the background uncertainty is the dominant source of error in regions of phase space that are enriched in $B \to X_c \ell^+ \nu_\ell$ (e.g., above $M_X \approx m_{D^0} = 1.86$ GeV). The exclusive $B \to X_u \ell^+ \nu_\ell$ modeling errors only contribute significantly in the resonance region at low M_X or high q^2. The full systematic and statistical correlations between all measured distributions are determined to allow for a future simultaneous analysis of all measured distributions, and are provided with the full systematic uncertainties of all measured distributions in Supplemental Material, Ref. [40].

The measured differential branching fractions as a function of E_ℓ^B, q^2, M_X, M_X^2, P_-, and P_+ are shown in Fig. 3 and the numerical values with full correlations can be found in Supplemental Material, Ref. [40]. The distributions are compared to the $B \to X_u \ell^+ \nu_\ell$ hybrid MC and the fully inclusive DFN [15] and BLNP [16] predictions with model parameters listed in Table I. All predictions are scaled to match the $B \to X_u \ell^+ \nu_\ell$ partial branching fraction ($\Delta\mathcal{B}$) with $E_\ell^B > 1$ GeV of $\Delta\mathcal{B} = 1.59 \times 10^{-3}$ from Ref. [1]. The uncertainty band of the hybrid prediction includes variations on the composition, form factors, and the inclusive modeling, whose central value is based on the DFN prediction but includes the difference to BLNP as an additional uncertainty. The agreement between the measured and predicted distributions is fair overall, with differences occurring for the fully inclusive predictions

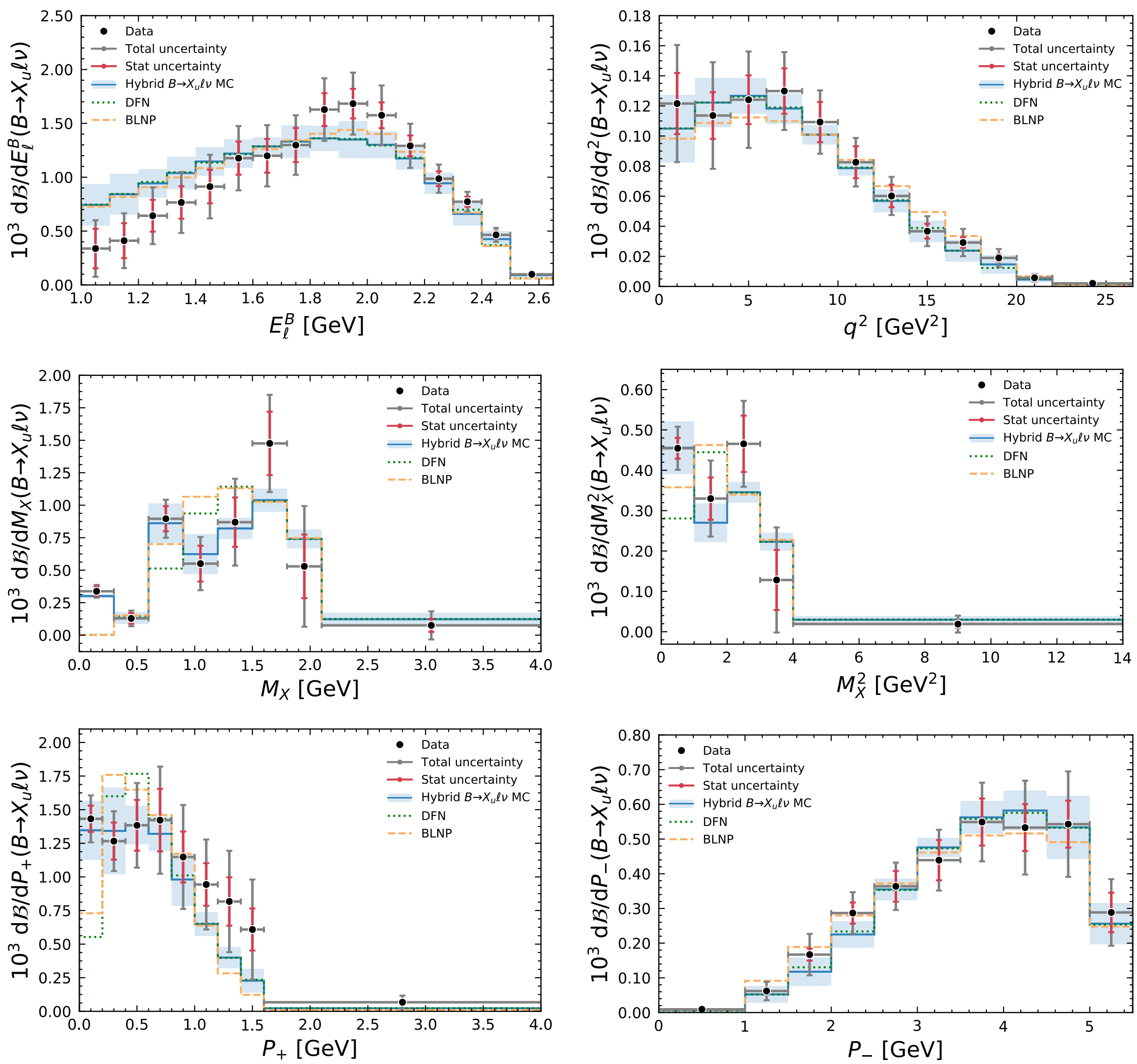

FIG. 3. The measured differential $B \to X_u \ell^+ \nu_\ell$ branching fractions are shown: the lepton energy in the B rest frame (E_ℓ^B), the four-momentum-transfer squared of the B to the X_u system [$q^2 = (p_B - p_X)^2$], the invariant hadronic mass and mass squared of the X_u system (M_X, M_X^2), and the light-cone momenta of the hadronic X_u system [$P_\pm = (E_X^B \mp |\mathbf{p}_X^B|)$]. The hybrid MC prediction and two inclusive calculations are also shown and scaled to $\Delta\mathcal{B} = 1.59 \times 10^{-3}$.

in the resonance region of, e.g., low M_X, and near the end point of q^2 and E_ℓ^B. There the hybrid MC describes the $B \to X_u \ell^+ \nu_\ell$ process more adequately due to the explicit inclusion of resonant contributions. The largest discrepancy is observed in E_ℓ^B, but the data points in the range of $E_\ell^B \in [1\text{–}1.8]$ GeV exhibit strong correlations and are only weakly correlated or anticorrelated with the other bins of the spectrum. To quantify the agreement with the three displayed predictions we carry out a χ^2 test using the experimental covariance only. We find a good χ^2 of 13.5 for the measured E_ℓ^B spectrum and the hybrid prediction with 16 degrees of freedom. Similarly we find for the DFN and BLNP predictions χ^2 values of 16.2 and 16.5, respectively.

In conclusion, this Letter presents the first measurements of differential branching fractions of inclusive semileptonic $B \to X_u \ell^+ \nu_\ell$ decays as a function of E_ℓ^B, q^2, M_X, M_X^2, P_-, and P_+ (a first preliminary measurement of the shape of the spectrum of M_X^2 was presented in Ref. [44] and Ref. [45] reported a differential branching fraction measurement as a function E_e^B, but without providing the full experimental uncertainties). The measurements use the full Belle data set of 711 fb^{-1} of integrated luminosity at the $\Upsilon(4S)$ resonance and for $\ell = e, \mu$ in which one of the two B mesons was fully reconstructed in hadronic modes. The differential branching fractions are obtained by subtracting $B \to X_c \ell^+ \nu_\ell$ and other backgrounds with the normalization determined by a fit to the M_X distribution of the hadronic X system. The resulting distributions are corrected for detector resolution and efficiency effects and unfolded to the phase space of the lepton energy of $E_\ell^B > 1$ GeV in the rest frame of the signal B meson. The measurements are, depending on the region of phase space, statistically or systematically limited, and show fair agreement to hybrid and inclusive predictions of $B \to X_u \ell^+ \nu_\ell$ decays. The measured distributions are sensitive to the shape function governing the nonperturbative dynamics of the $b \to u$ transition and will allow future direct determinations of the shape function and $|V_{ub}|$, as proposed by Refs. [6,7]. These novel analyses will provide new insights into the persistent tensions on the value of $|V_{ub}|$ from inclusive and exclusive determinations [8].

We thank Kerstin Tackmann, Frank Tackmann, Zoltan Ligeti, and Dean Robinson for discussions about the content of this manuscript. L. C., W. S., Rv. T., and F. B. were supported by the German Research Foundation (DFG) Emmy-Noether Grant No. BE 6075/1-1. L. C. was also supported by the Helmholtz W2/W3-116 grant. We thank the KEKB group for the excellent operation of the accelerator; the KEK cryogenics group for the efficient operation of the solenoid; and the KEK computer group, and the Pacific Northwest National Laboratory (PNNL) Environmental Molecular Sciences Laboratory (EMSL) computing group for strong computing support; and the National Institute of Informatics, and Science Information NETwork 5 (SINET5) for valuable network support. We acknowledge support from the Ministry of Education, Culture, Sports, Science, and Technology (MEXT) of Japan, the Japan Society for the Promotion of Science (JSPS), and the Tau-Lepton Physics Research Center of Nagoya University; the Australian Research Council including Grants No. DP180102629, No. DP170102389, No. DP170102204, No. DP150103061, No. FT130100303; Austrian Federal Ministry of Education, Science and Research (FWF) and FWF Austrian Science Fund No. P 31361-N36; the National Natural Science Foundation of China under Contracts No. 11435013, No. 11475187, No. 11521505, No. 11575017, No. 11675166, No. 11705209; Key Research Program of Frontier Sciences, Chinese Academy of Sciences (CAS), Grant No. QYZDJ-SSW-SLH011; the CAS Center for Excellence in Particle Physics (CCEPP); the Shanghai Pujiang Program under Grant No. 18PJ1401000; the Shanghai Science and Technology Committee (STCSM) under Grant No. 19ZR1403000; the Ministry of Education, Youth and Sports of the Czech Republic under Contract No. LTT17020; Horizon 2020 ERC Advanced Grant No. 884719 and ERC Starting Grant No. 947006 "InterLeptons" (European Union); the Carl Zeiss Foundation, the Deutsche Forschungsgemeinschaft, the Excellence Cluster Universe, and the VolkswagenStiftung; the Department of Atomic Energy (Project Identification No. RTI 4002) and the Department of Science and Technology of India; the Istituto Nazionale di Fisica Nucleare of Italy; National Research Foundation (NRF) of Korea Grants No. 2016R1D1A1B01010135, No. 2016R1-D1A1B02012900, No. 2018R1A2B3003643, No. 2018-R1A6A1A06024970, No. 2018R1D1A1B07047294, No. 2019K1A3A7A09033840, No. 2019R1I1A3A010-58933; Radiation Science Research Institute, Foreign Large-size Research Facility Application Supporting project, the Global Science Experimental Data Hub Center of the Korea Institute of Science and Technology Information and KREONET/GLORIAD; the Polish Ministry of Science and Higher Education and the National Science Center; the Ministry of Science and Higher Education of the Russian Federation, Agreement No. 14.W03.31.0026, and the HSE University Basic Research Program, Moscow; University of Tabuk research Grants No. S-1440-0321, No. S-0256-1438, and No. S-0280-1439 (Saudi Arabia); the Slovenian Research Agency Grants No. J1-9124 and No. P1-0135; Ikerbasque, Basque Foundation for Science, Spain; the Swiss National Science Foundation; the Ministry of Education and the Ministry of Science and Technology of Taiwan; and the United States Department of Energy and the National Science Foundation.

[*]cao@physik.uni-bonn.de
[†]florian.bernlochner@uni-bonn.de

[1] L. Cao *et al.* (Belle Collaboration), Phys. Rev. D **104**, 012008 (2021).

[2] M. Neubert, Phys. Rev. D **49**, 3392 (1994).
[3] P. Gambino and N. Uraltsev, Eur. Phys. J. C **34**, 181 (2004).
[4] C. W. Bauer, Z. Ligeti, M. Luke, A. V. Manohar, and M. Trott, Phys. Rev. D **70**, 094017 (2004).
[5] D. Benson, I. I. Bigi, and N. Uraltsev, Nucl. Phys. **B710**, 371 (2005).
[6] F. U. Bernlochner, H. Lacker, Z. Ligeti, I. W. Stewart, F. J. Tackmann, and K. Tackmann (SIMBA Collaboration), Phys. Rev. Lett. **127**, 102001 (2021).
[7] P. Gambino, K. J. Healey, and C. Mondino, Phys. Rev. D **94**, 014031 (2016).
[8] Y. S. Amhis *et al.* (HFLAV Collaboration), Eur. Phys. J. C **81**, 226 (2021).
[9] S. Kurokawa and E. Kikutani, Nucl. Instrum. Methods Phys. Res., Sect. A **499**, 1 (2003); and other papers included in this Volume; T. Abe *et al.*, Prog. Theor. Exp. Phys. **2013**, 03A001 (2013) and references therein.
[10] A. Abashian *et al.*, Nucl. Instrum. Methods Phys. Res., Sect. A **479**, 117 (2002); also see detector section in J. Brodzicka *et al.*, Prog. Theor. Exp. Phys. **2012**, 4D001 (2012).
[11] D. J. Lange, Nucl. Instrum. Methods Phys. Res., Sect. A **462**, 152 (2001).
[12] C. Ramirez, J. F. Donoghue, and G. Burdman, Phys. Rev. D **41**, 1496 (1990).
[13] M. Prim *et al.* (Belle Collaboration), Phys. Rev. D **101**, 032007 (2020).
[14] M. Prim, b2-hive/effort v0.1.0 (2020).
[15] F. De Fazio and M. Neubert, J. High Energy Phys. 06 (1999) 017.
[16] B. O. Lange, M. Neubert, and G. Paz, Phys. Rev. D **72**, 073006 (2005).
[17] T. Sjöstrand, Comput. Phys. Commun. **82**, 74 (1994).
[18] C. G. Boyd, B. Grinstein, and R. F. Lebed, Phys. Rev. Lett. **74**, 4603 (1995).
[19] B. Grinstein and A. Kobach, Phys. Lett. B **771**, 359 (2017).
[20] D. Bigi, P. Gambino, and S. Schacht, Phys. Lett. B **769**, 441 (2017).
[21] R. Glattauer *et al.* (Belle Collaboration), Phys. Rev. D **93**, 032006 (2016).
[22] E. Waheed *et al.* (Belle Collaboration), Phys. Rev. D **100**, 052007 (2019).
[23] F. U. Bernlochner and Z. Ligeti, Phys. Rev. D **95**, 014022 (2017).
[24] P. Zyla *et al.* (Particle Data Group), Prog. Theor. Exp. Phys. **2020**, 083C01 (2020).
[25] C. Bourrely, L. Lellouch, and I. Caprini, Phys. Rev. D **79**, 013008 (2009); **82**, 099902(E) (2010).
[26] J. A. Bailey, A. Bazavov, C. Bernard, C. M. Bouchard, C. DeTar *et al.* (Fermilab Lattice and MILC Collaborations), Phys. Rev. D **92**, 014024 (2015).
[27] Y. S. Amhis *et al.* (HFLAV Collaboration), Eur. Phys. J. C **81**, 226 (2021).
[28] G. Duplancic and B. Melic, J. High Energy Phys. 11 (2015) 138.
[29] F. U. Bernlochner, M. T. Prim, and D. J. Robinson, Phys. Rev. D **104**, 034032 (2021).
[30] A. Bharucha, J. High Energy Phys. 05 (2012) 092.
[31] A. Sibidanov *et al.* (Belle Collaboration), Phys. Rev. D **88**, 032005 (2013).
[32] J. P. Lees *et al.* (*BABAR* Collaboration), Phys. Rev. D **87**, 032004 (2013); **87**, 099904(E) (2013).
[33] P. del Amo Sanchez *et al.* (*BABAR* Collaboration), Phys. Rev. D **83**, 032007 (2011).
[34] M. Feindt, F. Keller, M. Kreps, T. Kuhr, S. Neubauer, D. Zander, and A. Zupanc, Nucl. Instrum. Methods Phys. Res., Sect. A **654**, 432 (2011).
[35] T. Chen and C. Guestrin, *Proceedings of the 22nd ACM SIGKDD International Conference on Knowledge Discovery and Data Mining KDD '16* (ACM, New York, 2016), 785, 10.1145/2939672.2939785.
[36] B. Efron, Ann. Stat. **7**, 1 (1979).
[37] K. G. Hayes, M. L. Perl, and B. Efron, Phys. Rev. D **39**, 274 (1989).
[38] A. Hocker and V. Kartvelishvili, Nucl. Instrum. Methods Phys. Res., Sect. A **372**, 469 (1996).
[39] T. Adye, in *Proceedings of the PHYSTAT 2011* (CERN, Geneva, 2011).
[40] See Supplemental Material at http://link.aps.org/supplemental/10.1103/PhysRevLett.127.261801 for additional details on this measurement including the split systematic uncertainties, the efficiency correction factors, the migration matrices, the experimental correlations of the measured differential spectra and the extracted first three moments, which includes Refs. [41–43].
[41] O. Buchmuller and H. U. Flacher, Phys. Rev. D **73**, 073008 (2006).
[42] M. Althoff *et al.* (TASSO Collaboration), Z. Phys. C **27**, 27 (1985).
[43] W. Bartel *et al.* (JADE Collaboration), Z. Phys. C **20**, 187 (1983).
[44] K. Tackmann (*BABAR* Collaboration), Eur. Phys. J. A **38**, 137 (2008).
[45] J. P. Lees *et al.* (*BABAR* Collaboration), Phys. Rev. D **95**, 072001 (2017).